mathematics

Article

Analytic Solution for Buckling Problem of Rectangular Thin Plates Supported by Four Corners with Four Edges Free Based on the Symplectic Superposition Method

Yushi Yang [1,2], Dian Xu [3], Jinkui Chu [1,2,*] and Rui Li [3]

1 Key Laboratory for Micro/Nano Technology and System of Liaoning Province, School of Mechanical Engineering, Dalian University of Technology, Dalian 116024, China; yangys@mail.dlut.edu.cn
2 State Key Laboratory of High-Performance Precision Manufacturing, School of Mechanical Engineering, Dalian University of Technology, Dalian 116024, China
3 State Key Laboratory of Structural Analysis, Optimization and CAE Software for Industrial Equipment, International Research Center for Computational Mechanics, School of Mechanics and Aerospace Engineering, Dalian University of Technology, Dalian 116024, China; dianxu@mail.dlut.edu.cn (D.X.); ruili@dlut.edu.cn (R.L.)
* Correspondence: chujk@dlut.edu.cn

Abstract: The buckling behavior of rectangular thin plates, which are supported at their four corner points with four edges free, is a matter of great concern in the field of plate and shell mechanics. Nevertheless, the complexities arising from the boundary conditions and governing equations present a formidable obstacle to the attainment of analytical solutions for these problems. Despite the availability of various approximate/numerical methods for addressing these challenges, the literature lacks accurate analytic solutions. In this study, we employ the symplectic superposition method, a recently developed method, to effectively analyze the buckling problem of rectangular thin plates analytically. These plates have four supported corners and four free edges. To achieve this, the problem is divided into two sub-problems and solve them separately using variable separation and symplectic eigen expansion, leading to analytical solutions. Finally, we obtain the resolution to the initial issue by superposing the sub-problems. The current solution method can be regarded as a logical, analytical, and rational approach as it begins with the basic governing equation and is systematically derived without assuming the forms of the solutions. To examine various aspect ratios and in-plane load ratios of rectangular thin plates, which are supported at their four corner points with four edges free, we provide numerical examples that demonstrate the buckling loads and typical buckling mode shapes.

Keywords: symplectic superposition method; rectangular thin plate; buckling; corner-point supports

MSC: 35E05; 74K20; 74G60

check for updates

Citation: Yang, Y.; Xu, D.; Chu, J.; Li, R. Analytic Solution for Buckling Problem of Rectangular Thin Plates Supported by Four Corners with Four Edges Free Based on the Symplectic Superposition Method. *Mathematics* **2024**, *12*, 249. https://doi.org/10.3390/math12020249

Academic Editors: Shujin Laima, Xiaowei Jin, Hehe Ren and Yong Cao

Received: 16 November 2023
Revised: 27 December 2023
Accepted: 8 January 2024
Published: 12 January 2024

1. Introduction

The mechanics of plates and shells have been studied by many scholars [1,2]. Rectangular plates supported by corner point are commonly used in various engineering applications, including building structures, mechanical components, and aerospace vehicles. The buckling of plates is a significant mechanical failure that has received extensive attention in recent decades. At present, many scholars have studied the buckling problem of plates. Obtaining analytical solutions for such buckling problems is crucial for both theoretical understanding and practical applications. The primary aim of conducting linear buckling analysis on plates is to establish the buckling load and its associated buckling mode. These parameters serve as crucial indicators for structural design, offering valuable reference values. Obtaining analytical solutions is often challenging due to the intricate nature of the mathematical equations and boundary conditions. Current analytical solutions for the buckling phenomenon in rectangular plates are primarily restricted to scenarios featuring uncomplicated boundary conditions with two opposite sides simply supported, commonly referred to as Lévy type plates. As for rectangular plates with non-opposite side simple supported, most research has relied on similar/numerical methods [3–12]. For rectangular plates under corner support conditions, finite difference method [13], differential quadrature method [14,15], discrete singular convolution method [16,17], meshless method [18], generalized Galerkin method [19,20], etc., have been used to obtain the similar/numerical solution of the buckling problem of such plates. Consequently, there is a scarcity of reports on analytical methods and analytical solutions for these specific cases.

The introduction of symplectic mathematical concepts into elasticity by Academician Zhong [21–23] has revolutionized the field of elastic mechanics solutions. This innovative approach, known as symplectic elasticity, has been widely applied in various areas such as structural folds [24], fractures [25], and elastic waves [26]. Over the years, researchers like Li et al. [27] have further developed this concept and introduced the symplectic superposition method for complex plate-shell mechanics. This novel analytical method has provided solutions to bending, vibration, and stability problems in plate-shell structures. Instead of utilizing the conventional Lagrange system rooted in Euclidean space, the symplectic superposition method functions within the Hamiltonian system embedded in symplectic space. The basic idea of symplectic superposition method is as follows: the problem to be solved is introduced into Hamilton system to form the boundary value problem of Hamilton dual equation; The original problem is divided into several sub-problems. For these sub-problems, the corresponding eigenvalue problems are constructed by symplectic mathematical method, and the eigenvalue solutions are obtained analytically. Then, the control variables such as deflection (bending problem), mode (vibration problem) or buckling mode (stability problem) are accurately characterized by means of symplectic eigenvalue expansion. The solution of the original problem is obtained by solving the superposition subproblem. The symplectic superposition method offers a significant benefit in that it offers a direct solution approach devoid of any predetermined functions. This approach demonstrates utmost rationality. It combines the advantages of the symplectic-mathematical method, which does not need to assume the solution form in advance, and the programmatic advantages of the Superposition method, which has a unified mathematical structure and is not limited by the specific type of problem. This method overcomes the problems of separating variables and the failure of the semi-inverse method (such as Rayleigh-Ritz method) encountered in the solution process of the other traditional methods, and at the same time, circumvents the problems of failing to analytically solve eigenvalue equations, which are caused by the use of the traditional symplectic-mathematical method. This approach overcomes challenges associated with solving eigenequations and offers distinct benefits in analyzing vibration and buckling problems in plates and shells with complex boundaries. so that the method demonstrates a unique advantage in analytically solving the problems of plate and shell dynamics, providing a fresh theoretical tool for obtaining new analytic solutions in various plate-related problems such as static bending, vibration, and buckling. Additionally, the technique offers efficient convergence, surpassing some conventional methods. Through the utilization of this approach, the scientists successfully obtained precise and comprehensive analytical solutions without making any assumptions regarding the structure of the solution. This particular advantage distinguishes it from the traditional semi-inverse method. Notably, up until now, the utilization of the symplectic superposition method has been exclusively focused on addressing vibration issues associated with rectangular plates.

The primary objective of this research is to address the problem of buckling of a rectangular thin plate, which are supported at their four corner points with four edges free, which is notorious for its complex boundary conditions. To assess the effectiveness of the proposed method, this study examines the buckling behavior of rectangular plates with different aspect ratios and load ratios. The obtained results consistently exhibit a significant level of concurrence with the findings derived from an extensive finite element analysis.

This verification effectively verifies both the precision of the proposed method and the analytical solution.

If the edge boundary condition is changing, for instance, FSFS, or SSSS, CCCC, the analytical solution will change. Different superposition systems need to be constructed for plate buckling problems with different boundaries. The buckling problem of plates with different boundary conditions has been studied by Li et al. [27]. It is worth mentioning that although the primary focus of this study revolves around linear problems, there is potential for tackling nonlinear problems concerning plates with significant deformation by employing the symplectic superposition method in conjunction with the perturbation method [28–30]. Such attempts will be made in the follow-up studies.

The main novelty of the SSM lies in the Hamiltonian framework to solve higher-order partial differential equations. This method distinguishes itself by decomposing the problem into two subproblems and utilizing advanced techniques in symplectic space, such as variable separation and symplectic eigen expansion, to derive analytical solutions. Unlike traditional semi-inverse methods, the SSM does not rely on predetermined assumptions, enhancing its robustness and applicability. Furthermore, our work addresses new analytical solutions under non-Lévy-type boundary conditions (BCs), a complex issue in previous research. This breakthrough demonstrates the SSM's capability to tackle challenging mathematical characteristics, thereby presenting a significant advancement in the field and offering a valuable benchmark for comparing and evaluating other methods.

The symplectic superposition method can be applied to other geometric plates, e.g., triangular, circular, polygonal. If the geometries of the plate are changing, we need to construct different symplectic superposition systems and derive new formulas. The exact solution procedure can be seen in "On the symplectic superposition method for analytic free vibration solutions of right triangular plates" [31] Circular plates have been studied using the symplectic method, the details can be found at "Natural vibration of circular and annular thin plates by Hamiltonian approach" [32] and "The dynamic behavior of circular plates under impact loads" [33]. We are currently conducting some research on the use of symplectic superposition for irregularly shaped plates (plates with a rectangular central cutout and L-shaped plates) "New analytic free vibration solutions of plates with a rectangular central cutout by symplectic superposition" "New analytic free vibration solutions of L-shaped moderately thick plates by symplectic superposition" which are being submitted for publication.

Since The elastic stiffness D is used as a constant parameter in my solution, this method is still valid if it is discretized and used as a variable stiffness matrix in my solution. It is only necessary to combine the region decomposition method to dis-perse the plate into multiple regions, assign different stiffness to different sub-regions, and meet the continuity conditions at the joints of each sub-region, and combine the boundary conditions of the plate to obtain the solution of the mechanical problem of the plate.

2. Governing Equations and Eigenproblems of Hamilton System for Rectangular Thin Plate Buckling Problem

By utilizing the variational principle associated with Hellinger-Reissner variables and the Lagrange multiplier technique [34], the buckling phenomenon of thin plates can be characterized within the specified domain through the ensuing variational principle [27]:

$$\begin{aligned}\delta\Pi_H &= \delta\iint\limits_{\Omega}\left\{\frac{D}{2}\left(\frac{\partial^2 w}{\partial x^2}\right)^2+\frac{D}{2}\left(\frac{\partial\theta}{\partial y}\right)^2+T\left(\theta-\frac{\partial w}{\partial y}\right)+D\nu\frac{\partial^2 w}{\partial x^2}\frac{\partial\theta}{\partial y}+D(1-\nu)\left(\frac{\partial\theta}{\partial x}\right)^2\right.\\ &\left.-\frac{D}{2(1-\nu^2)}\left(\frac{M_y}{D}+\frac{\partial\theta}{\partial y}+\nu\frac{\partial^2 w}{\partial x^2}\right)^2+\frac{1}{2}\left[P_x\left(\frac{\partial w}{\partial x}\right)^2+P_y\theta^2\right]\right\}dxdy\\ &=0\end{aligned} \tag{1}$$

where Π_H is the Hamiltonian functional, Ω denotes the plate domain, w is the transverse displacement of the plate midplane, T is the Lagrangian multiplier, θ is an introduced quantity, D is the flexural rigidity ($D = Eh^3/\left[12\left(1-\nu^2\right)\right]$), h is the plate thickness, E is the elastic modulus, ν is the Poisson's ratio, M_y is the bending moments ($M_y = -D\left(\partial^2 w/\partial y^2 + \nu \partial^2 w/\partial x^2\right)$), P_x and P_y is normal membrane forces.

Assuming the independence of w, θ, T, and M_y, and the arbitrariness of their variation, Equation (1) yields:

$$\begin{aligned} \frac{\partial w}{\partial y} &= \theta \\ \frac{\partial \theta}{\partial y} &= -\nu \frac{\partial^2 w}{\partial x^2} - \frac{M_y}{D} \\ \frac{\partial T}{\partial y} &= -D\left(1-\nu^2\right)\frac{\partial^4 w}{\partial x^4} + \nu \frac{\partial^2 M_y}{\partial x^2} + P_x \frac{\partial^2 w}{\partial x^2} \\ \frac{\partial M_y}{\partial y} &= -T + 2D(1-\nu)\frac{\partial^2 \theta}{\partial x^2} - P_y \theta \end{aligned} \tag{2}$$

It is noted from first and the last equation of Equation (2) that $\theta = \partial w/\partial y$, and $T = -V_y$, where V_y is the equivalent shear force, which could be expressed as:

$$V_y = Q_y + \frac{\partial M_{xy}}{\partial x} + P_y \frac{\partial w}{\partial y} \tag{3}$$

Therefore, the matrix equation that represents the homogeneous governing equation for the expansion of a thin plate can be formulated as:

$$\frac{\partial \mathbf{Z}}{\partial y} = \mathbf{HZ} \tag{4}$$

where $\mathbf{Z} = [w, \theta, T, M_y]^{\mathrm{T}}$, $\boldsymbol{H}=\begin{bmatrix} \boldsymbol{F} & \boldsymbol{G} \\ \boldsymbol{Q} & -\boldsymbol{F}^{\mathrm{T}} \end{bmatrix}$, $\boldsymbol{F} = \begin{bmatrix} 0 & 1 \\ -\nu\partial^2/\partial x^2 & 0 \end{bmatrix}$, $\boldsymbol{G} = \begin{bmatrix} 0 & 0 \\ 0 & -1/D \end{bmatrix}$, $\boldsymbol{Q} = \begin{bmatrix} -D\left(1-\nu^2\right)\frac{\partial^4}{\partial x^4} + P_x \frac{\partial^2}{\partial x^2} & 0 \\ 0 & \frac{2D(1-\nu)\partial^2}{\partial x^2} - P_y \end{bmatrix}$.

$\mathbf{H}$ is the Hamiltonian operator matrix, which satisfy $\mathbf{H}^{\mathrm{T}} = \mathbf{JHJ}$, where $\mathbf{J} = \begin{bmatrix} 0 & \mathbf{I}_2 \\ -\mathbf{I}_2 & 0 \end{bmatrix}$ is the symplectic matrix [21] where $\mathbf{I}_2$ is the 2×2 unit matrix.

Equation (4) is solved by the method of separating variables

$$\mathbf{Z} = \mathbf{X}(x)Y(y) \tag{5}$$

where $\mathbf{X}(x) = \left[w(x), \theta(x),\ T(x),\ M_y\ (x)\right]^{\mathrm{T}}$ is a unary vector of x and $Y(y)$ is a unary function of y. By substituting Equation (5) into Equation (4), we can get:

$$dY(y)/dy = \mu Y(y) \tag{6}$$

$$\mathbf{HX}(x) = \mu \mathbf{X}(x) \tag{7}$$

in which $\mathbf{X}(x)$ and μ are the eigenvector and eigenvalue of the Hamiltonian matrix $\mathbf{H}$, respectively. The characteristic equation corresponding to Equation (7):

$$\begin{vmatrix} -\mu & 1 & 0 & 0 \\ -\nu\lambda^2 & -\mu & 0 & -\frac{1}{D} \\ P_x\lambda^2 - D\lambda^4\left(1-\nu^2\right) & 0 & -\mu & \nu\lambda^2 \\ 0 & -P_y + 2D\lambda^2(1-\nu) & -1 & -\mu \end{vmatrix} = 0 \tag{8}$$

Expanding Equation (8), we get

$$D\left(\lambda^2 + \mu^2\right)^2 = P_x\lambda^2 + P_y\mu^2 \tag{9}$$

The solution to this equation is

$$\begin{aligned} \lambda_{1,2} &= \pm a_1 i \\ \lambda_{3,4} &= \pm a_2 i \end{aligned} \tag{10}$$

where $a_1 = \sqrt{\mu^2 - P_x/(2D) + \sqrt{P_x^2 + 4D\mu^2(P_y - P_x)}/(2D)}$, $a_2 = \sqrt{\mu^2 - P_x/(2D) - \sqrt{P_x^2 + 4D\mu^2(P_y - P_x)}/(2D)}$.

The eigen-solution of $w(x)$ could be obtained:

$$w(x) = A\cos(a_1 x) + B\sin(a_1 x) + C\cos(a_2 x) + F\sin(a_2 x) \tag{11}$$

where the constants A, B, C and F are undetermined coefficients which could be obtained by the boundary conditions

3. Analytic Buckling Solutions of Rectangular Thin Plates Supported by Four Corners with Four Edges Free

In order to tackle the concern of buckling in a thin plate supported by four corners with four edges free, we initially obtain the analytical solution for a fundamental subproblem utilizing the symplectic method. Subsequently, we utilize the superposition method to derive the analytical solution for the primary problem. As demonstrated in Figure 1, the symplectic superposition diagram portrays the established coordinate system with the origin positioned at one corner of the plate. The length and width of the plate are denoted as 'a' and 'b' respectively. The left and upper edges of the plate determine the orientation of the ox and oy axes, as illustrated in Figure 1a. In order to effectively tackle the initial problem, it is divided into two subproblems, as shown in Figure 1b,c. Corner support is represented by 'P', freedom by 'F', and simply supported by 'S'.

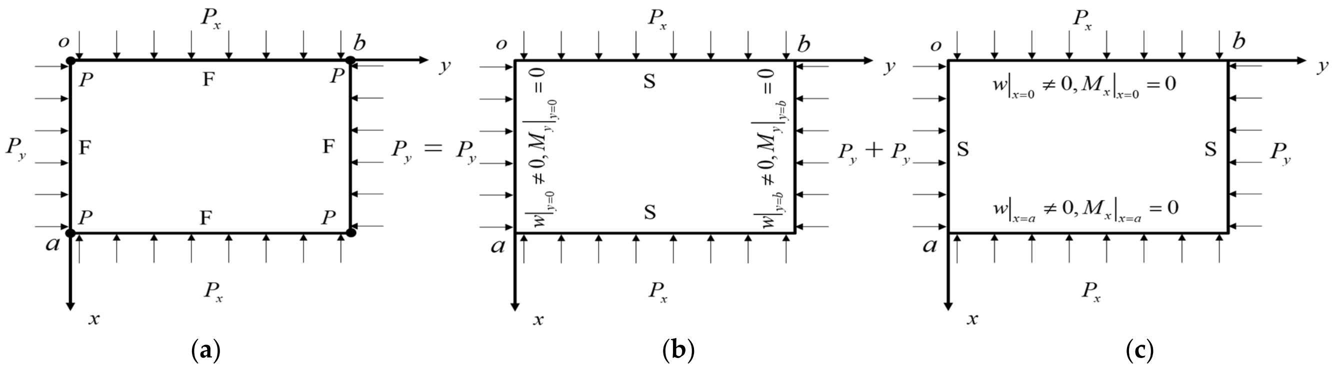

Figure 1. Symplectic superposition for buckling problem of rectangular thin plates supported by four corners with four edges free (**a**) Symplectic superposition for the whole problem (**b**) Symplectic superposition for the subproblem (1) (**c**) Symplectic superposition for the subproblem (2).

The boundary condition of the original problem is to satisfy the point-supported boundary condition at the four corner points, i.e.,

$$w|_{(0,0),(0,b),(a,0),(a,b)} = 0 \tag{12}$$

On the four edges of the plate, the free boundary conditions need to be satisfied, i.e.:

$$\begin{aligned} V_y|_{y=0,b} = 0,\ M_y|_{y=0,b} = 0 \\ V_x|_{x=0,a} = 0,\ M_x|_{x=0,a} = 0 \end{aligned} \tag{13}$$

The plates in both subproblems have initial boundary conditions that are simply supported on all four sides. These boundary conditions must be fulfilled:

$$\begin{aligned} w|_{y=0,b} = 0,\ M_y\big|_{y=0,b} = 0 \\ w|_{x=0,a} = 0,\ M_x|_{x=0,a} = 0 \end{aligned} \tag{14}$$

On this basis, displacements expressed in terms of $\sum_{m=1,2,3,\ldots}^{\infty} \kappa 1_m \sin(\alpha_m x)$ and $\sum_{m=1,2,3,\ldots}^{\infty} \kappa 2_m \sin(\alpha_m x)$ are applied to the $y = 0$ and $y = b$ sides of the plate in subproblem (1), respectively; displacements expressed in terms of $\sum_{n=1,2,3,\ldots}^{\infty} \kappa 3_n \sin(\beta_n y)$ and $\sum_{n=1,2,3,\ldots}^{\infty} \kappa 4_n \sin(\beta_n y)$ are applied to the $x = 0$ and $x = a$ sides of the plate in subproblem (2), where $\alpha_m = m\pi/a$, $\beta_n = n\pi/b$, $\kappa 1_m$, $\kappa 2_m$, $\kappa 3_n$ and $\kappa 4_n$ are the parameters to be determined ($m = 1,2,3,\ldots$, $n = 1,2,3,\ldots$).

The subproblem (1) represented in Figure 1b is first solved as an example. For a rectangular thin plate simply supported on $x = 0$ and $x = a$ the boundary conditions on those sides need require:

$$w(x)|_{x=0,a} = w''(x)\big|_{x=0,a} = 0 \tag{15}$$

By plugging Equation (11) into Equation (15), we obtain a set of equations that contains the coefficients that need to be determined. If we assume all constants are set to zero (to eliminate the possibility of buckling), it is crucial for the determinant of the coefficient matrix to be zero. As a result, the following equation can be derived:

$$\sin(aa_1)\sin(aa_2) = 0 \tag{16}$$

Its roots are:

$$a_{1,2} = \pm\frac{m\pi}{a} \tag{17}$$

where $m = 1,2,3,\ldots,$

Thus, the eigenvalue can be solved:

$$\begin{aligned} \mu_{m1,m2} = \pm\sqrt{\frac{P_y}{2D} + \alpha_m^2 - \frac{\sqrt{P_y^2 + 4D\alpha_m^2\left(P_y - P_x\right)}}{2D}} \\ \mu_{m3,m4} = \pm\sqrt{\frac{P_y}{2D} + \alpha_m^2 + \frac{\sqrt{P_y^2 + 4D\alpha_m^2\left(P_y - P_x\right)}}{2D}} \end{aligned} \tag{18}$$

and eigenvectors:

$$\mathbf{X}_{mi} = \sin(\alpha_m x)\begin{Bmatrix} 1 \\ \mu_{mi} \\ -\mu_{mi}\gamma_{mi} \\ D\left(\nu\alpha_m^2 - \mu_{mi}^2\right) \end{Bmatrix} \tag{19}$$

where $\gamma_{mi} = P_y - D\left[\mu_{mi}^2 - \alpha_m^2(2-\nu)\right](i = 1,2,3,4)$.

In this subproblem, the state vector can be expressed as:

$$\mathbf{Z} = \sum_{m=1}^{\infty}\sum_{i=1}^{4} C_{mi} e^{\mu_{mi} y}\mathbf{X}_{mi} \tag{20}$$

where the value of the constant "$C_{mi}(m = 1,2,3,\ldots,i = 1,2,3,4)$" can be determined based on the boundary conditions of the given direction. As previously discussed, upon dividing the original problem into subproblems, it is essential to enforce displacement in the direction of subproblem (1). The appropriate boundary conditions for this are as follows:

$$\begin{aligned} w|_{y=0} = \sum_{m=1,2,3,\ldots}^{\infty} \kappa 1_m \sin(\alpha_m x),\ M_y\big|_{y=0} = 0 \\ w|_{y=b} = \sum_{m=1,2,3,\ldots}^{\infty} \kappa 2_m \sin(\alpha_m x),\ M_y\big|_{y=b} = 0 \end{aligned} \tag{21}$$

Substituting Equation (20) into Equation (21) yields the modal displacement expression of subproblem (1)

$$\begin{aligned} w_1(\overline{x},\overline{y}) &= a \sum_{m=1,2,3,\ldots}^{\infty} \frac{\sin(m\pi\overline{x})}{\xi_m^2-\varsigma_m^2} \\ &\times\left\{\operatorname{csc}\mathrm{h}(\phi\varsigma_m)\left(\xi_m^2-m^2\pi^2 v\right)\left\{\overline{\kappa 2}_m \mathrm{sh}(\phi\varsigma_m\overline{y})+\overline{\kappa 1}_m \mathrm{sh}[\phi\varsigma_m(1-\overline{y})]\right\}\right. \\ &\left.-\operatorname{csc}\mathrm{h}(\phi\xi_m)\left(\varsigma_m^2-m^2\pi^2 v\right)\left\{\overline{\kappa 2}_m \mathrm{sh}(\phi\xi_m\overline{y})+\overline{\kappa 1}_m \mathrm{sh}[\phi\xi_m(1-\overline{y})]\right\}\right\} \end{aligned} \tag{22}$$

where $\overline{y}=y/b$, $\overline{x}=x/a$, $\overline{\kappa 1}_m=\kappa 1_m/a$, $\overline{\kappa 2}_m=\kappa 2_m/a$, $\phi=b/a$, $\xi_m=a\mu_{m1}$, $\varsigma_m=a\mu_{m3}$.

For subproblem (2) represented in Figure 1c, the solution process is similar to that of subproblem (1), and the modal displacement of the corresponding plate is:

$$\begin{aligned} & w_2(\overline{x},\overline{y}) = b \sum_{n=1,2,3,\ldots}^{\infty} \frac{\sin(n\pi\overline{y})}{\tilde{\xi}_n^2-\tilde{\varsigma}_n^2} \\ &\times\left\{\operatorname{csc}\mathrm{h}\left(\tilde{\phi}\tilde{\varsigma}_n\right)\left(\tilde{\xi}_n^2-n^2\pi^2 v\right)\left\{\mathrm{sh}\left(\tilde{\phi}\tilde{\varsigma}_n\overline{x}\right)\overline{\kappa 4}_n+\mathrm{sh}\left[\tilde{\phi}\tilde{\varsigma}_n(1-\overline{x})\right]\overline{\kappa 3}_n\right\}\right. \\ &\left.-\operatorname{csc}\mathrm{h}\left(\tilde{\phi}\tilde{\xi}_n\right)\left(\tilde{\varsigma}^2{}_n-n^2\pi^2\nu\right)\left\{\mathrm{sh}\left(\tilde{\phi}\tilde{\xi}_n\overline{x}\right)\overline{\kappa 4}_n+\mathrm{sh}\left[\tilde{\phi}\tilde{\xi}_n(1-\overline{x})\right]\overline{\kappa 3}_n\right\}\right\} \end{aligned} \tag{23}$$

where $\overline{\kappa 3}_n=\kappa 3_n/b$, $\overline{\kappa 4}_n=\kappa 4_n/b$, $\tilde{\xi}_n=b\mu_{n1}$, $\tilde{\varsigma}_n=b\mu_{n3}$, $\tilde{\phi}=a/b$, $\mu_{n1}=\sqrt{P_x/(2D)+\beta_n^2-\sqrt{P_x^2+4D\beta_n^2\left(P_x-P_y\right)}/(2D)}$, $\mu_{n3}=\sqrt{P_x/(2D)+\beta_n^2+\sqrt{P_x^2+4D\beta_n^2\left(P_x-P_y\right)}/(2D)}$.

Through the utilization of the derivation mentioned above, we are able to acquire the modal displacement solutions for the two subproblems. This in turn allows for the derivation of various other physical quantities, such as bending moments and angles, using a similar approach. The establishment of the equivalence between the superposition of the subproblems and the original problem is essential for determining the constant $\kappa 1_m$, $\kappa 2_m$, $\kappa 3_n$ and $\kappa 4_n$.

It is necessary to satisfy the boundary conditions at the four corner points of the rectangular plate, such that the displacement of these corner points becomes zero after the subproblems are superimposed. Irrespective of the values assumed by the pending parameters $\kappa 1_m$, $\kappa 2_m$, $\kappa 3_n$ and $\kappa 4_n$ the displacement of the corner points is already satisfied.

Similarly, the requirement for the four free edges in terms of $y=0$, $y=b$, $x=0$ and $x=a$ adherence to zero bending moment and equivalent shear force is also fulfilled after the subproblems are superimposed. Consequently, the zero bending moment condition has been met, leaving only the need to fulfill the boundary conditions related to equivalent shear force.

For the edges $y=0$, superimpose the equivalent shear forces along the $y=0$ edges of the two subproblems so that the sum is 0, i.e., $V_y\big|_{y=0}=\sum_{i=1}^2 V_y^i\Big|_{y=0}=0$, which simplifies to the first set of equations:

$$\begin{aligned} &\frac{1}{\xi_m^2-\varsigma_m^2} \\ &\times\left\{\varsigma_m\left(\xi_m^2-m^2\pi^2\nu\right)\operatorname{csc}\mathrm{h}(\phi\varsigma_m)\left[\overline{\kappa 2}_m-\overline{\kappa 1}_m\mathrm{ch}(\phi\varsigma_m)\right]\left[\overline{R}-\varsigma_m{}^2+m^2\pi^2(2-\nu)\right]\right. \\ &\left.-\xi_m\left(\varsigma_m{}^2-m^2\pi^2\nu\right)\operatorname{csc}\mathrm{h}(\phi\xi_m)\left[\overline{\kappa 2}_m-\overline{\kappa 1}_m\mathrm{ch}(\phi\xi_m)\right]\left[\overline{R}-\xi_m{}^2+m^2\pi^2(2-\nu)\right]\right\} \\ &+\sum_{n=1,2,3,\ldots}^{\infty}\frac{2mn\pi^2}{\tilde{\xi}_n{}^2-\tilde{\varsigma}_n{}^2}\left[\overline{\kappa 3}_n-\cos(m\pi)\overline{\kappa 4}_n\right] \\ &\times\left\{\frac{\left(\tilde{\xi}_n{}^2-n^2\pi^2\nu\right)\left[n^2\pi^2+\phi^2\overline{R}-\tilde{\varsigma}_n{}^2(2-\nu)\right]}{\tilde{\varsigma}_n{}^2+m^2\pi^2\phi^2}-\frac{\left(\tilde{\varsigma}_n{}^2-n^2\pi^2\nu\right)\left[n^2\pi^2+\phi^2\overline{R}-\tilde{\xi}_n{}^2(2-\nu)\right]}{\tilde{\xi}_n{}^2+m^2\pi^2\phi^2}\right\}=0 \end{aligned} \tag{24}$$

where $\overline{R}=a^2P_y/D$ $(m=1,2,3,\cdots)$.

For the edges $y = b$, superimpose the equivalent shear forces along the $y = b$ edges of the two subproblems so that the sum is 0, i.e., $V_y\big|_{y=b} = \sum_{i=1}^{2} V_y^i\Big|_{y=b} = 0$, which simplifies to the second set of equations:

$$\begin{aligned}
&\frac{1}{\xi_m^2 - \varsigma_m^2} \\
&\times\left\{\varsigma_m\left(\xi_m^2 - m^2\pi^2\nu\right)\operatorname{csc\,h}(\phi\varsigma_m)\left[\overline{\kappa 1}_m - \overline{\kappa 2}_m \operatorname{ch}(\phi\varsigma_m)\right]\left[\overline{R} - {\varsigma_m}^2 + m^2\pi^2(2-\nu)\right]\right. \\
&\left.-\xi_m\left({\varsigma_m}^2 - m^2\pi^2\nu\right)\operatorname{csc\,h}(\phi\xi_m)\left[\overline{\kappa 1}_m - \overline{\kappa 2}_m \operatorname{ch}(\phi\xi_m)\right]\left[\overline{R} - {\xi_m}^2 + m^2\pi^2(2-\nu)\right]\right\} \\
&-\sum_{n=1,2,3,\ldots}^{\infty} \frac{2mn\pi^2}{\widetilde{\xi}_n{}^2 - \widetilde{\varsigma}_n{}^2}\left[\overline{\kappa 3}_n - \cos(m\pi)\overline{\kappa 4}_n\right] \\
&\times\left\{\frac{\left(\widetilde{\xi}_n{}^2 - n^2\pi^2\nu\right)\left[n^2\pi^2 + \phi^2\overline{R} - \widetilde{\varsigma}_n{}^2(2-\nu)\right]}{\widetilde{\varsigma}_n{}^2 + m^2\pi^2\phi^2} - \frac{\left(\widetilde{\varsigma}_n{}^2 - n^2\pi^2\nu\right)\left[n^2\pi^2 + \phi^2\overline{R} - \widetilde{\xi}_n{}^2(2-\nu)\right]}{\widetilde{\xi}_n{}^2 + m^2\pi^2\phi^2}\right\} = 0
\end{aligned} \tag{25}$$

For the edges $x = 0$, superimpose the equivalent shear forces along the $x = 0$ edges of the two subproblems so that the sum is 0, i.e., $V_x\big|_{x=0} = \sum_{i=1}^{2} V_x^i\Big|_{x=0} = 0$, which simplifies to the third set of equations:

$$\begin{aligned}
&\frac{1}{\widetilde{\xi}_n^2 - \widetilde{\varsigma}_n{}^2} \\
&\times\left\{\widetilde{\varsigma}_n \operatorname{csc\,h}\left(\widetilde{\phi}\widetilde{\varsigma}_n\right)\left(\widetilde{\xi}_n{}^2 - n^2\pi^2 v\right)\left[\overline{\kappa 4}_n - \overline{\kappa 3}_n \operatorname{ch}\left(\widetilde{\phi}\widetilde{\varsigma}_n\right)\right]\left[\widetilde{R} - \widetilde{\varsigma}_n{}^2 + n^2\pi^2(2-v)\right]\right. \\
&\left.-\widetilde{\xi}_n \operatorname{csc\,h}\left(\widetilde{\phi}\widetilde{\xi}_n\right)\left(\widetilde{\varsigma}_n^2 - n^2\pi^2\nu\right)\left[\overline{\kappa 4}_n - \overline{\kappa 3}_n \operatorname{ch}\left(\widetilde{\phi}\widetilde{\xi}_n\right)\right]\left[\widetilde{R} - \widetilde{\xi}_n{}^2 + n^2\pi^2(2-\nu)\right]\right\} \\
&+\sum_{m=1,2,3,\ldots}^{\infty} \frac{2nm\pi^2}{\xi_m^2 - \varsigma_m^2}\left[\overline{\kappa 1}_m - \cos(n\pi)\overline{\kappa 2}_m\right] \\
&\times\left\{\frac{\left(\xi_m^2 - m^2\pi^2 v\right)\left[m^2\pi^2 + \widetilde{\phi}^2\widetilde{R} - \varsigma_m^2(2-v)\right]}{\varsigma_m^2 + n^2\pi^2\widetilde{\phi}^2} - \frac{\left(\varsigma_m^2 - m^2\pi^2 v\right)\left[m^2\pi^2 + \widetilde{\phi}^2\widetilde{R} - \xi_m^2(2-v)\right]}{{\xi_m}^2 + n^2\pi^2\widetilde{\phi}^2}\right\} = 0
\end{aligned} \tag{26}$$

For the edges $x = a$, superimpose the equivalent shear forces along the $x = a$ edges of the two subproblems so that the sum is 0, i.e., $V_x\big|_{x=a} = \sum_{i=1}^{2} V_x^i\Big|_{x=a} = 0$, which simplifies to the fourth set of equations:

$$\begin{aligned}
&\frac{1}{\widetilde{\xi}_n^2 - \widetilde{\varsigma}_n{}^2} \\
&\times\left\{\widetilde{\varsigma}_n \operatorname{csc\,h}\left(\widetilde{\phi}\widetilde{\varsigma}_n\right)\left(\widetilde{\xi}_n{}^2 - n^2\pi^2 v\right)\left[\overline{\kappa 3}_n - \overline{\kappa 4}_n \operatorname{ch}\left(\widetilde{\phi}\widetilde{\varsigma}_n\right)\right]\left[\widetilde{R} - \widetilde{\varsigma}_n{}^2 + n^2\pi^2(2-v)\right]\right. \\
&\left.-\widetilde{\xi}_n \operatorname{csc\,h}\left(\widetilde{\phi}\widetilde{\xi}_n\right)\left(\widetilde{\varsigma}_n^2 - n^2\pi^2\nu\right)\left[\overline{\kappa 3}_n - \overline{\kappa 4}_n \operatorname{ch}\left(\widetilde{\phi}\widetilde{\xi}_n\right)\right]\left[\widetilde{R} - \widetilde{\xi}_n{}^2 + n^2\pi^2(2-\nu)\right]\right\} \\
&-\sum_{m=1,2,3,\ldots}^{\infty} \frac{2nm\pi^2}{\xi_m^2 - \varsigma_m^2}\left[\overline{\kappa 1}_m - \cos(n\pi)\overline{\kappa 2}_m\right] \\
&\times\left\{\frac{\left(\xi_m^2 - m^2\pi^2 v\right)\left[m^2\pi^2 + \widetilde{\phi}^2\widetilde{R} - \varsigma_m^2(2-v)\right]}{\varsigma_m^2 + n^2\pi^2\widetilde{\phi}^2} - \frac{\left(\varsigma_m^2 - m^2\pi^2 v\right)\left[m^2\pi^2 + \widetilde{\phi}^2\widetilde{R} - \xi_m^2(2-v)\right]}{{\xi_m}^2 + n^2\pi^2\widetilde{\phi}^2}\right\} = 0
\end{aligned} \tag{27}$$

Equations (24)–(27) represent an infinite set of coupled equations, yet they can be reduced to a finite number of terms $m = 1, 2, 3, \cdots nt$, $n = 1, 2, 3, \cdots nt$ when the plate experiences buckling. In order for formula (24)–(27) to have a non-zero solution, it is necessary for the coefficients $\kappa 1_m$, $\kappa 2_m$, $\kappa 3_n$ and $\kappa 4_n$ to not all be zero, thereby satisfying the condition of the joint equation. The aforementioned condition results in the determination of the coefficient matrix being zero in the system of equations, which ultimately establishes the buckling load. By solving for the buckling load, the non-zero solution to the system of equations can be obtained, and by substituting these values back into Equations (22) and (23) and summing up, the corresponding buckling mode can be determined. Mathematica, a mathematical analysis tool developed by Wolfram, Inc. in the USA, is used to obtain the free vibration solutions and the corresponding modal shapes during the analysis of the symplectic superposition method.

4. Comprehensive Buckling Loads and MS Results

In Figures 2 and 3, the buckling loads of rectangular thin plates supported by four corners with four edges free are presented. These plates have aspect ratios of 1 and 2, respectively. The load ratio ranges from 0 to 5, and a Poisson's ratio of 0.3 is assumed. Throughout the comparison process, we utilize the widely accepted FEM integrated in the ABAQUS 2017 software package to compare with our analytical solutions. The thickness-to-width ratio of the plates is fixed at 10^{-6} a. We employ the 4-node thin shell element S4R and maintain a uniform mesh size equal to $1/100$ a of the plate width through the linear perturbation procedure. It is evident that the current results align closely with the finite element results. In Figure 4, the first ten order buckling modes of the rectangular thin plates supported by four corners with four edges free are displayed for the case where $b/a = 1$ and $P_x/P_y = 1$. In Figure 5, the first ten order buckling modes of the rectangular thin plates supported by four corners with four edges free are displayed for the case where $b/a = 2$ and $P_x/P_y = 1$. By conducting comparisons, it is discovered that the symplectic superposition method can accurately calculate the buckling modes as well. Overall, these examples provide compelling evidence to support the validity of the proposed method and the accuracy of the analytical results. The color indicates the current magnitude of the modal displacement, red indicates the maximum value of the displacement, blue indicates the minimum value of the displacement (absolute maximum).

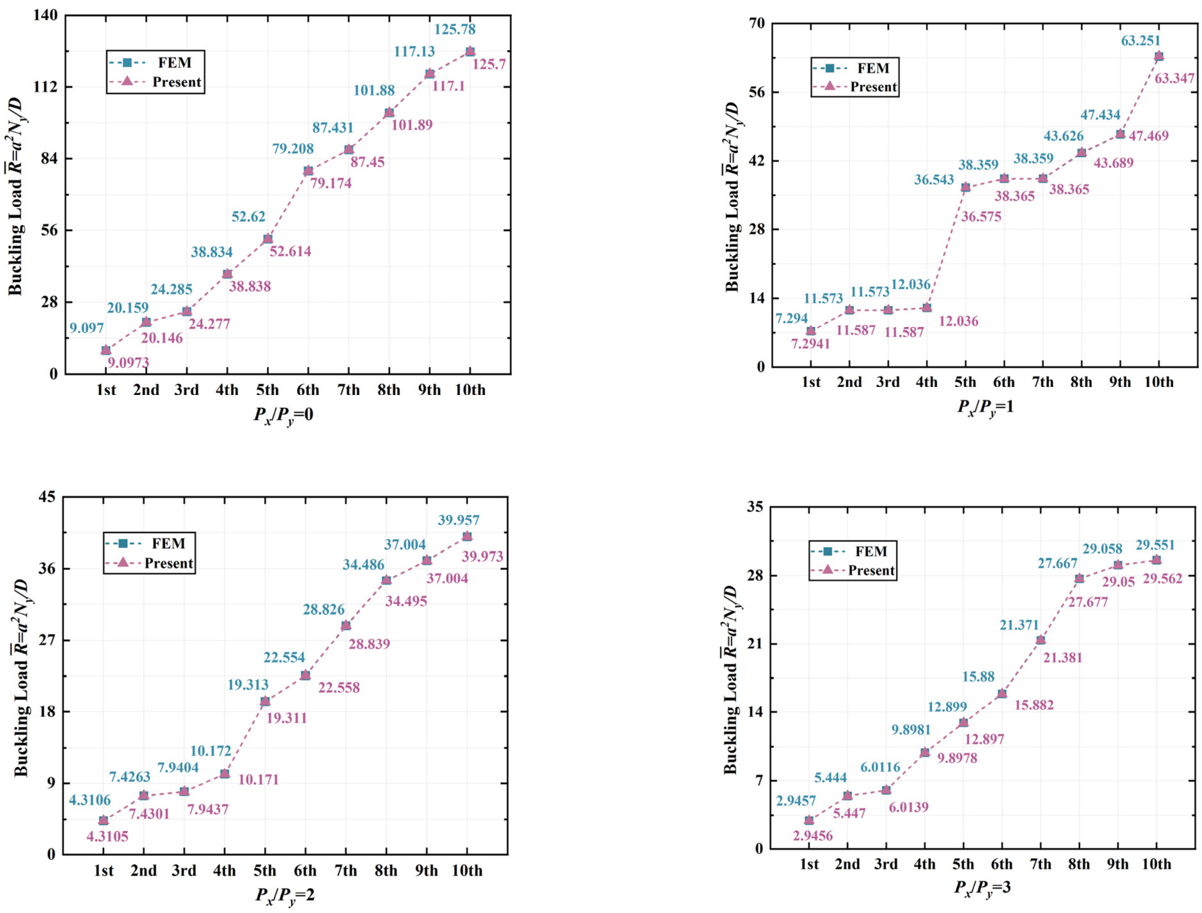

Figure 2. *Cont.*

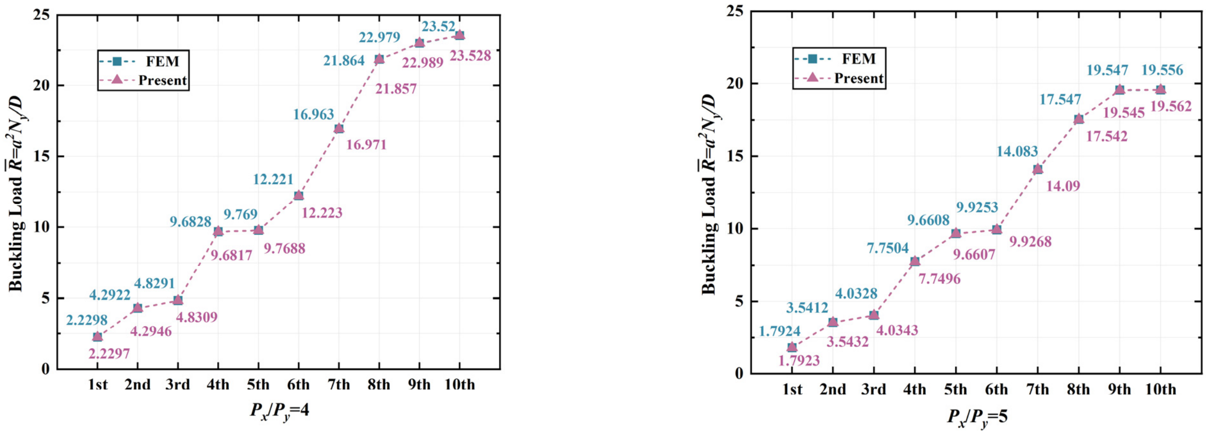

Figure 2. First ten buckling loads, R, of the plates under different $b/a = 1$.

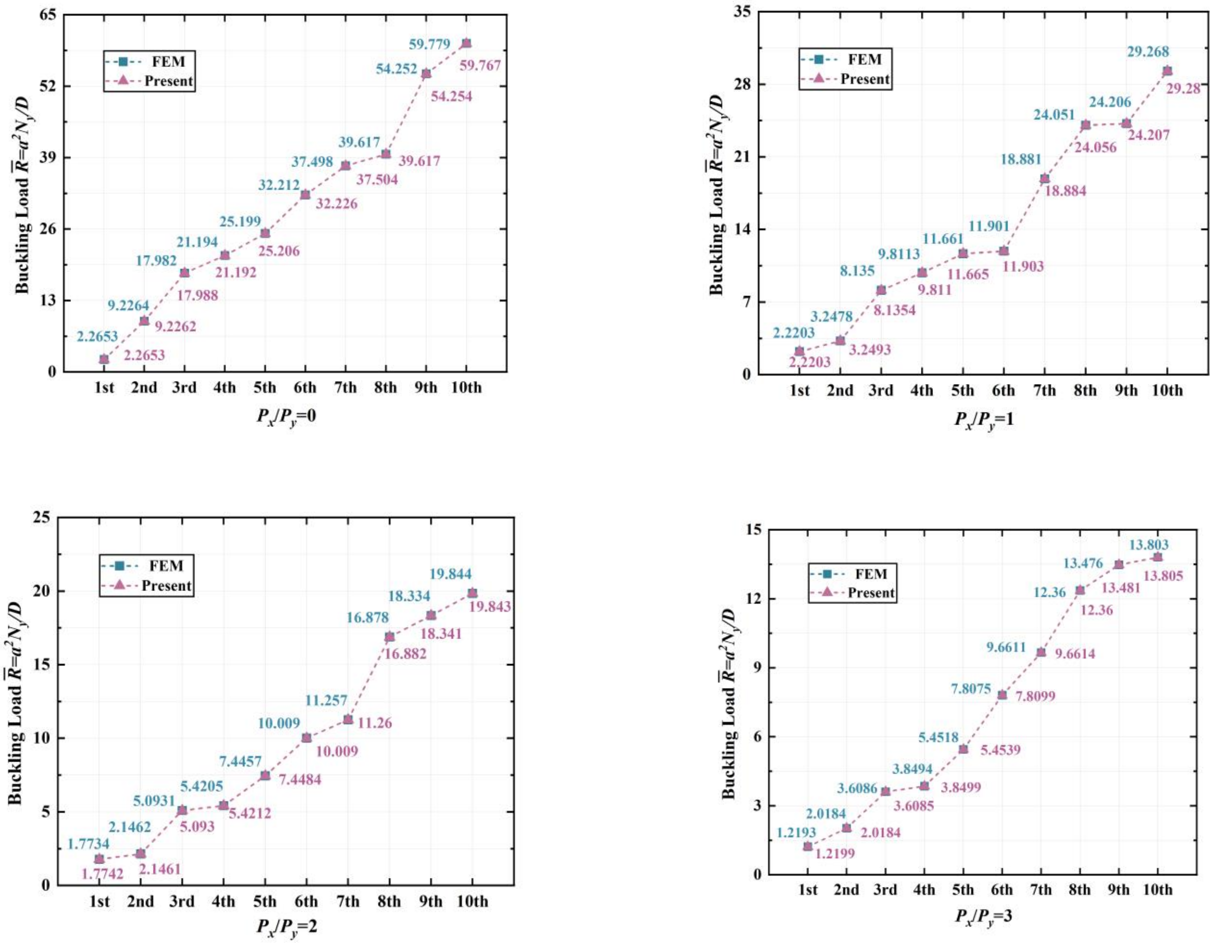

Figure 3. *Cont.*

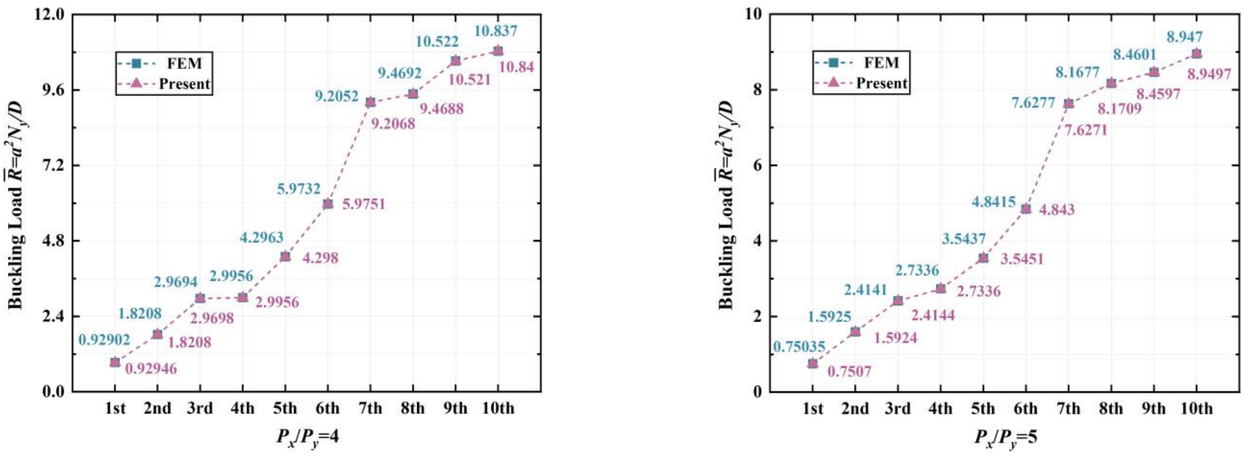

Figure 3. First ten buckling loads, $\overline{R}$, of the plates under different $b/a = 2$.

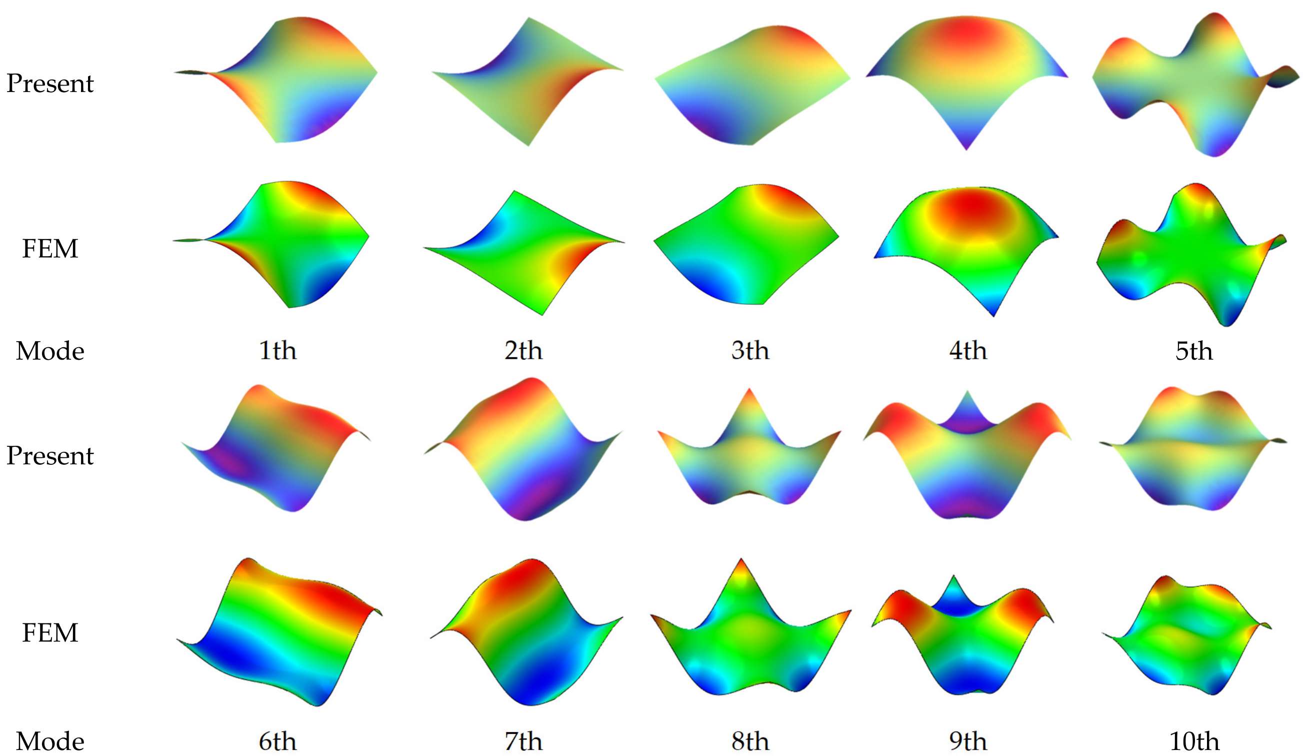

Figure 4. First ten buckling modes of the plates under $P_x/P_y = 1$, with $b/a = 1$.

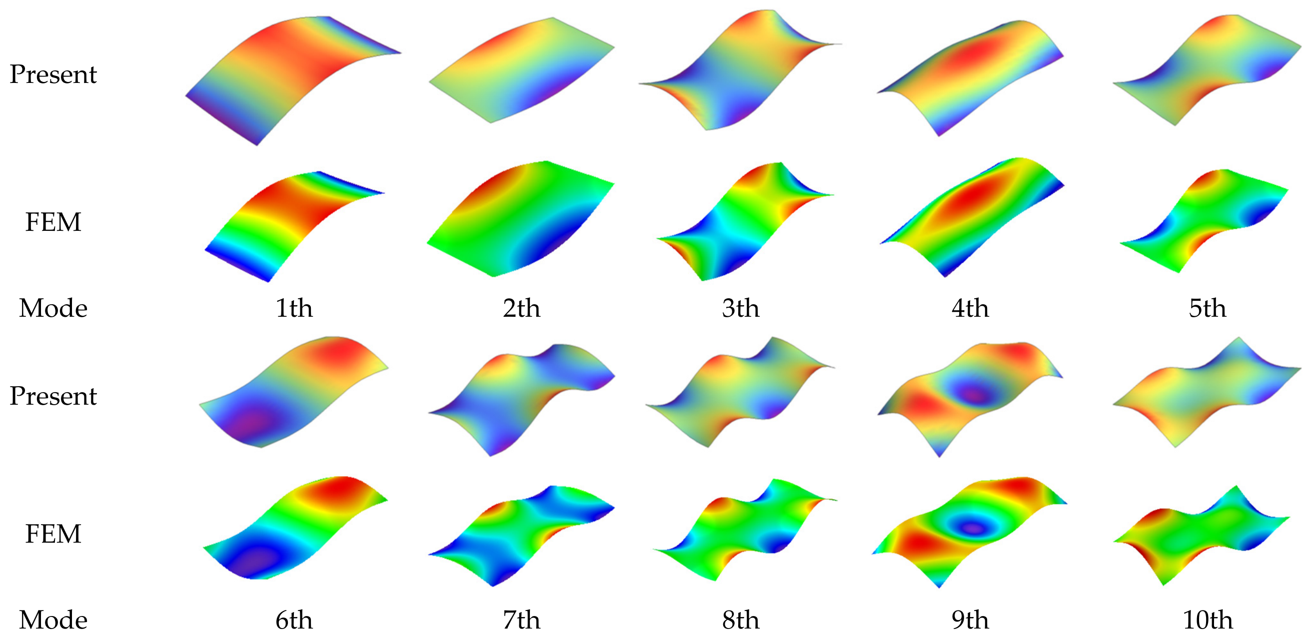

Figure 5. First ten buckling modes of the plates under $P_x/P_y = 1$, with $b/a = 2$.

5. Conclusions

In this study, we propose a new analytical solution for analyzing the buckling behavior of a rectangular thin plate that is supported at its four corner points with four edges free and subjected to both unidirectional and bidirectional in-plane loads. The symplectic superposition method is employed for this purpose. This solution provides comprehensive information on the buckling load and buckling mode analysis, considering varying aspect ratios and load ratios. These results can be used as a valuable reference for the comparison and evaluation of other approximate or numerical methods. The symplectic superposition method is advantageous as it does not make any assumptions about the form of the solution, ensuring a rigorous analytical derivation from beginning to end. As a result, this method has the potential to be extended further and apply to the derivation of new analytical solutions for complex plate and shell problems.

Author Contributions: Conceptualization, methodology, writing—original draft preparation, software, formal analysis, Y.Y.; methodology, validation, D.X.; funding acquisition, project administration, J.C.; supervision, R.L. All authors have read and agreed to the published version of the manuscript.

Funding: This research was funded by National Natural Science Foundation of China (grant number 52175265 and 52275281) and the Fundamental Research Funds for the Central Universities (grant number DUT21ZD101, DUT21GF308 and DUT20LAB303).

Data Availability Statement: Data are contained within the article.

Conflicts of Interest: The authors declare no conflict of interest.

References

1. Zhang, J.; Lu, J.; Ullah, S.; Gao, Y.; Zhao, D. Buckling analysis of rectangular thin plates with two opposite edges free and others rotationally restrained by finite Fourier integral transform method. *Zamm—J. Appl. Math. Mech. Z. Für Angew. Math. Mech.* **2021**, *101*, e202000153. [CrossRef]
2. Nguyen, T.N.; Zhang, D.; Mirrashid, M.; Nguyen, D.K.; Singhatanadgid, P. Fast analysis and prediction approach for geometrically nonlinear bending analysis of plates and shells using artificial neural networks. *Mech. Adv. Mater. Struct.* **2023**, 1–19. [CrossRef]
3. Civalek, Ö. Application of differential quadrature (DQ) and harmonic differential quadrature (HDQ) for buckling analysis of thin isotropic plates and elastic columns. *Eng. Struct.* **2004**, *26*, 171–186. [CrossRef]
4. Hu, Z.; Zheng, X.; An, D.; Zhou, C.; Yang, Y.; Li, R. New analytic buckling solutions of side-cracked rectangular thin plates by the symplectic superposition method. *Int. J. Mech. Sci.* **2021**, *191*, 106051. [CrossRef]

5. Jafari, N.; Azhari, M. Buckling of moderately thick arbitrarily shaped plates with intermediate point supports using a simple hp-cloud method. *Appl. Math. Comput.* **2017**, *313*, 196–208. [CrossRef]
6. Liew, K.M.; Chen, X.L.; Reddy, J.N. Mesh-free radial basis function method for buckling analysis of non-uniformly loaded arbitrarily shaped shear deformable plates. *Comput. Methods Appl. Mech. Eng.* **2004**, *193*, 205–224. [CrossRef]
7. Sakata, T.; Hosokawa, K. Vibrations of clamped orthotropic rectangular plates. *J. Sound Vib.* **1988**, *3*, 429–439. [CrossRef]
8. Shi, G. Flexural vibration and buckling analysis of orthotropic plates by the boundary element method. *Int. J. Solids Struct.* **1990**, *12*, 1351–1370. [CrossRef]
9. Ungbhakorn, V.; Singhatanadgid, P. Buckling analysis of symmetrically laminated composite plates by the extended Kantorovich method. *Compos. Struct.* **2006**, *73*, 120–128. [CrossRef]
10. Zhang, Y.X.; Yang, C.H. Recent developments in finite element analysis for laminated composite plates. *Compos. Struct.* **2009**, *88*, 147–157. [CrossRef]
11. Van Do, V.N.; Chang, K.H.; Lee, C. Post-buckling analysis of FGM plates under in-plane mechanical compressive loading by using a mesh-free approximation. *Arch. Appl. Mech.* **2019**, *89*, 1421–1446. [CrossRef]
12. Syngellakis, S.; Elzein, A. Plate buckling loads by the boundary element method. *Int. J. Numer. Methods Eng.* **1994**, *37*, 1763–1778. [CrossRef]
13. Ravari, M.R.K.; Shahidi, A.R. Axisymmetric buckling of the circular annular nanoplates using finite difference method. *Meccanica* **2013**, *48*, 135–144. [CrossRef]
14. Moradi, S.; Taheri, F. Application of differential quadrature method to the delamination buckling of composite plates. *Comput. Struct.* **1999**, *70*, 615–623. [CrossRef]
15. Wang, X.; Tan, M.; Zhou, Y. Buckling analyses of anisotropic plates and isotropic skew plates by the new version differential quadrature method. *Thin Wall. Struct.* **2003**, *41*, 15–29. [CrossRef]
16. Civalek, O.; Yavas, A. Discrete singular convolution for buckling analyses of plates and columns. *Struct. Eng. Mech.* **2008**, *29*, 279–288. [CrossRef]
17. Civalek, O.; Korkmaz, A.; Demir, C. Discrete singular convolution approach for buckling analysis of rectangular Kirchhoff plates subjected to compressive loads on two-opposite edges. *Adv. Eng. Softw.* **2010**, *41*, 557–560. [CrossRef]
18. Wang, J.; Liew, K.M.; Tan, M.J.; Rajendran, S. Analysis of rectangular laminated composite plates via FSDT meshless method. *Int. J. Mech. Sci.* **2002**, *44*, 1275–1293. [CrossRef]
19. Lopatin, A.V.; Morozov, E.V. Approximate buckling analysis of the CCFF orthotropic plates subjected to in-plane bending. *Int. J. Mech. Sci.* **2014**, *85*, 38–44. [CrossRef]
20. Wang, D.; Peng, H. A Hermite reproducing kernel Galerkin meshfree approach for buckling analysis of thin plates. *Comput. Mech.* **2013**, *51*, 1013–1029. [CrossRef]
21. Zhong, W. Method of Separation of Variables and Hamiltonian System. *Comput. Struct. Mech. Appl.* **1991**, *8*, 229–240. (In Chinese)
22. Zhong, W. A New Systematic Methodology for Theory of Elasticity. Dalian University of Technology Press: Dalian, China, 1995.
23. Yao, W.; Zhong, W. *Symplectic Elasticity*; Higher Education Press: Beijing, China, 2002.
24. Zhang, T. Symplectic analysis for wrinkles, A case study of layered neo-hookean structures. *J. Comput. Appl. Math.* **2017**, *84*, 071002. [CrossRef]
25. Xu, X.S.; Zhou, Z.H.; Leung, A.Y.T. Analytical stress intensity factors for edge-cracked cylinder. *Int. J. Mech. Sci.* **2010**, *52*, 892–903. [CrossRef]
26. Ma, Y.; Zhang, Y.; Kennedy, D. A symplectic analytical wave-based method for the wave propagation and steady state forced vibration of rectangular thin plates. *J. Sound Vib.* **2015**, *339*, 196–214. [CrossRef]
27. Li, R.; Wang, H.; Zheng, X.; Xiong, S.; Hu, Z.; Yan, X.; Xiao, Z.; Xu, H.; Li, P. New analytic buckling solutions of rectangular thin plates with two free adjacent edges by the symplectic superposition method. *Eur. J. Mech. A Solids* **2019**, *76*, 247–262. [CrossRef]
28. Hutter, K.; Olunloyo, V.O.S. Vibration of an anisotropically prestressed thick rectangular membrane with small bending rigidity. *Acta. Mech.* **1974**, *20*, 1–22. [CrossRef]
29. Hutter, K.; Olunloyo, V.O.S. Vibration of a prestressed orthotropic rectangular thin plate via singular perturbation technique. *Acta. Mech.* **1986**, *64*, 165–178.
30. Chien, W.; Pan, L.; Liu, X. Large deflection problem of a clamped elliptical plate subjected to uniform pressure. *Appl. Math. Mech.* **1992**, *10*, 891–908.
31. Yang, Y.; An, D.; Xu, H.; Li, P.; Wang, B.; Li, R. On the symplectic superposition method for analytic free vibration solutions of right triangular plates. *Arch. Appl. Mech.* **2021**, *91*, 187–203. [CrossRef]
32. Zhou, Z.H.; Wong, K.W.; Xu, X.S.; Leung, A.Y.T. Natural vibration of circular and annular thin plates by Hamiltonian approach. *J. Sound Vib.* **2011**, *330*, 1005–1017. [CrossRef]
33. Tseng, W.D.; Tarn, J.Q. Exact elasticity solution for axisymmetric deformation of circular plates. *J. Mech.* **2015**, *31*, 617–629. [CrossRef]
34. Qian, W. *Variational Method and Finite Element Method*; Science Press: Beijing, China, 1980.